Available online at www.sciencedirect.com

ScienceDirect

Energy Procedia 63 (2014) 4313 – 4322

Energy Procedia

GHGT-12

Preparing for CO_2 storage in the Arctic – Assessing background seismic activity and noise characteristics at the CO2 Lab site, Svalbard

D. Kühn[a]*, V. Oye[a], J. Albaric[a], D. Harris[b], G. Hillers[c], A. Braathen[d], S. Olaussen[e]

[a]*NORSAR, Gunnar Randers vei 15, 2007 Kjeller, Norway*
[b]*Deschutes Signal Processing LLC, 81211 E Wapinitia Road, Maupin, OR 97037, USA*
[c]*Institut des Sciences de la Terre, Université Joseph Fourier, Grenoble, France*
[d]*Department of Geosciences, University of Oslo, Sem Sælands vei 1, 0371 Oslo, Norway*
[e]*Department of Arctic Geology, The University Centre in Svalbard, P.O. Box 156, 9171 Longyearbyen, Norway*

Abstract

Due to its remoteness, the CO2 Lab close to the town of Longyearbyen on Svalbard presents a unique opportunity to demonstrate the entire CO_2 value chain based on its closed energy system. The formation considered as potential CO_2 storage unit consists of mixed sandstone and shale beds, presenting itself as a fractured, low-permeability reservoir. A geophone network surrounding the injection well has been installed to locate microseismic events during injection tests and to estimate background seismicity. During the first water injection in 2010, a microseismic event (M ~ 1) was recorded and located close to the injection well, followed by a series of aftershocks. Later injection tests did not generate any detectable microseismic events; nevertheless, pressure and flow rate showed a pattern characteristic for fracture opening potentially indicating "aseismic" fracture propagation. Records of ambient seismic noise are analysed by a cross-correlation method in order to reconstruct the impulse functions between sensors. The daily cross-correlations are dominated by tube wave signals originating from the bottom of the well showing a sudden increase of activity. We also demonstrate a noise cancellation method exhibiting great potential towards cancellation of electromagnetic and cultural noise. Albeit several difficulties that were approached at the CO2 Lab, new knowledge and guidelines for best practice containment monitoring using seismic methods in the Arctic could be developed.

Peer-review under responsibility of the Organizing Committee of GHGT-12

Keywords: CO_2 sequestration; microseismic monitoring; ambient seismic noise; cross-correlation; Arctic

* Corresponding author. Tel.: +47-63805-900; fax: +47-63805-901.
E-mail address: daniela@norsar.no

Peer-review under responsibility of the Organizing Committee of GHGT-12
doi:10.1016/j.egypro.2014.11.467

1. Introduction

Since 2007, CO_2 Capture and Storage (CCS) research has been carried out in the Longyearbyen CO2 Lab (hosted by the University Centre in Svalbard, UNIS) and a spin-off company (UNIS CO2-lab AS). Longyearbyen is the largest settlement in the Svalbard archipelago and one of the world's northernmost towns. Due to its remoteness, it presents a unique opportunity to demonstrate the entire CO_2 value chain based on its closed energy system including coal mines, a coal fuelled power plant and geological structures suited for CO_2 sequestration.

The Svalbard archipelago is located in the northwestern margin of the Barents Sea Shelf. The in-situ CCS research site is located in Adventdalen, 5 km outside the town of Longyearbyen. The valley of Adventdalen is situated on the north-eastern flank of the Spitsbergen Central Tertiary Basin, which constitutes a foreland basin formed during the West Spitsbergen orogeny as a result of the Tertiary opening of the North Atlantic [2]. Within the basin, strata dip to the southwest (1 - 3°), thus, the reservoir layer, situated at a depth of 670-970 m at the injection site, outcrops at a distance of 15-20 km towards the northeast [1].

The CO_2 storage unit, i.e. the reservoir, consists of stacked sandstones of the Upper Triassic and Middle Jurassic age (De Gerdaalen and Knorringfjellet formations) deposited in a paralic to shallow marine environment of which the topmost part is significantly condensed. The primary caprock is formed by a 400 m thick layer of Jurassic and Lower Cretaceous shales; the Agardhfjellet and Rurikfjellet formations, respectively, whereas the impermeable near-surface layer of permafrost may constitute a secondary top-seal [2].

Eight wells were drilled from the permafrost overburden down to a maximum of about 1000 m depth in order to analyze the composition and the structure of the reservoir, to perform injection tests and to deploy instruments close to the reservoir. To gain a preliminary map of the geomechanical properties of the reservoir, multiple measurements were performed (2D seismic surveys, well logs, downhole microseismic monitoring, vertical seismic profiling, tracer tests and gas samples). Although the reservoir sandstone exhibits a low primary permeability (max 1-2 mD) and porosity (5-18%), injection test campaigns, ranging from high-rate/short-time leak-off tests (LOT) to lower-rate/longer-time step-rate tests (SRT), demonstrate injectivity especially in the lower part of the reservoir (870-970 m), indicating an unconventional, fractured reservoir [2]. Surprisingly, the reservoir pressure is sub-hydrostatic, strengthening the confidence in the overlying shales to act as a seal [2].

2. Microseismic monitoring

Several recent studies have demonstrated that microseismic monitoring is a powerful and cost-effective tool within a suite of CO_2 containment monitoring methods. E.g. at the industrial-scale CO_2 capture and storage project at In Salah, Algeria, microseismic monitoring revealed occurrence of several thousand microearthquakes associated with the CO_2 injection [3] and proved valuable to cluster and characterize microseismic events. Already in 2010, a high-frequency geophone network surrounding the injection well had been established at the Longyearbyen CO2 Lab through the SafeCO2 project with the purpose to detect and locate microseismic events. The geophone network was then upgraded in the subsequent years and consists since 2013 of two borehole strings (a 5-level 3C geophone string deployed in the observation well Dh3 down to a depth of 300 m and an 8-level geophone string deployed in the injection borehole Dh4 down to a depth of 590 m, both with a 50 m level spacing) and 5 3C geophones positioned in shallow wells (12 m depth). One challenge for the data analysis is that the records of seismicity induced by (water) injection have to be separated from signals resulting from frequent local mining operations, icequakes and regional earthquakes. Permafrost poses another challenge, especially for the receivers that are placed on or close to the surface. Although permafrost reaches down to about 150 m depth, some parts of the partially overpressured, unconsolidated fluvial sediments (upper 60-80 m) seem to be fluidized. This became evident when mud was ejecting from two shallow wells during drilling. Other indications are that the geophones deployed at 12 m depth show highly attenuated S-wave signals as compared with the P-wave signals and with the S-wave signals that are recorded below the permafrost layer [4]. Also results from an active S-wave seismic source experiment and an 80 m deep [5], fully cored permafrost well (Dh8) indicate low shear strengths in the uppermost 60 m [6].

Deployment of geophones to monitor induced microseismicity are therefore preferably installed below the permafrost.

During the first water injection in 2010, a microseismic event (M ~ 1) was recorded and located close to the injection well, followed by a series of 7 aftershocks identified using a matched filter method based on normalized cross-correlation [7]. Later injection tests did not generate any detectable microseismic events [4]; nevertheless, pressure and flow rate showed a pattern characteristic for fracture opening potentially indicating "aseismic" fracture propagation or slow slip. Such slow slip events may contribute considerably to enhance fluid transport and could explain the often observed gap between the extent of newly created fractures as calculated by reservoir engineers from pressure fall-off curves and the stimulated reservoir volume as interpreted from microseismic observations (e.g. [8]; [9]).

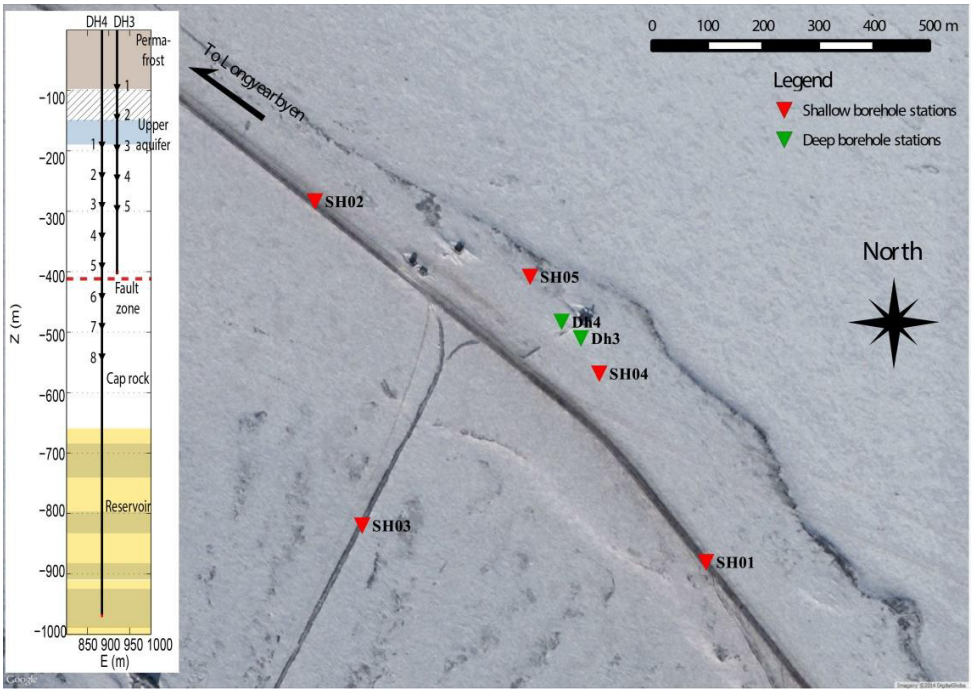

Fig. 1. Microseismic monitoring network at the UNIS CO2 Lab; red triangles: yellow borehole stations; green triangles: heads of wells equipped with geophone strings (see inlet for depth position of sensors; schematic geological depth section after [2], Fig. 15).

3. Ambient seismic noise cross-correlations

Since the permanent microseismic monitoring network at the Longyearbyen CO2 Lab is recording in a continuous mode, we possess records of ambient seismic noise since 2010. Recent results have shown that cross-correlation of the ambient seismic noise field between different sensors leads to the reconstruction of the impulse function between these sensors ("Green's functions", e.g. [10]) and can be used to track the temporal evolution of the crustal properties ([11], [12]). The main advantages of this new monitoring method are that it does not require active seismic sources and thus is very economic, that velocity changes are measured continuously and that the level of accuracy in measuring seismic velocity changes is unprecedented [13].

Before applying any analysis, we quality controlled the recordings of all stations carefully. In this process, we detected numerous seismic signals recorded within well Dh4. These signals started to occur rather suddenly on the 24th of November 2013 at approximately 09:40h and their number increased over the following days. Fig. 2 (a-c) displays helicorder plots for the 24th of November, the 28th of November and the 10th of December. By that time, the

detection of any other signals (e.g. from regional or local events) amidst these very short transient signals became noticeably difficult. The sudden onset of this activity is also clearly visible in a change of frequency content in the data (Fig. 2d).

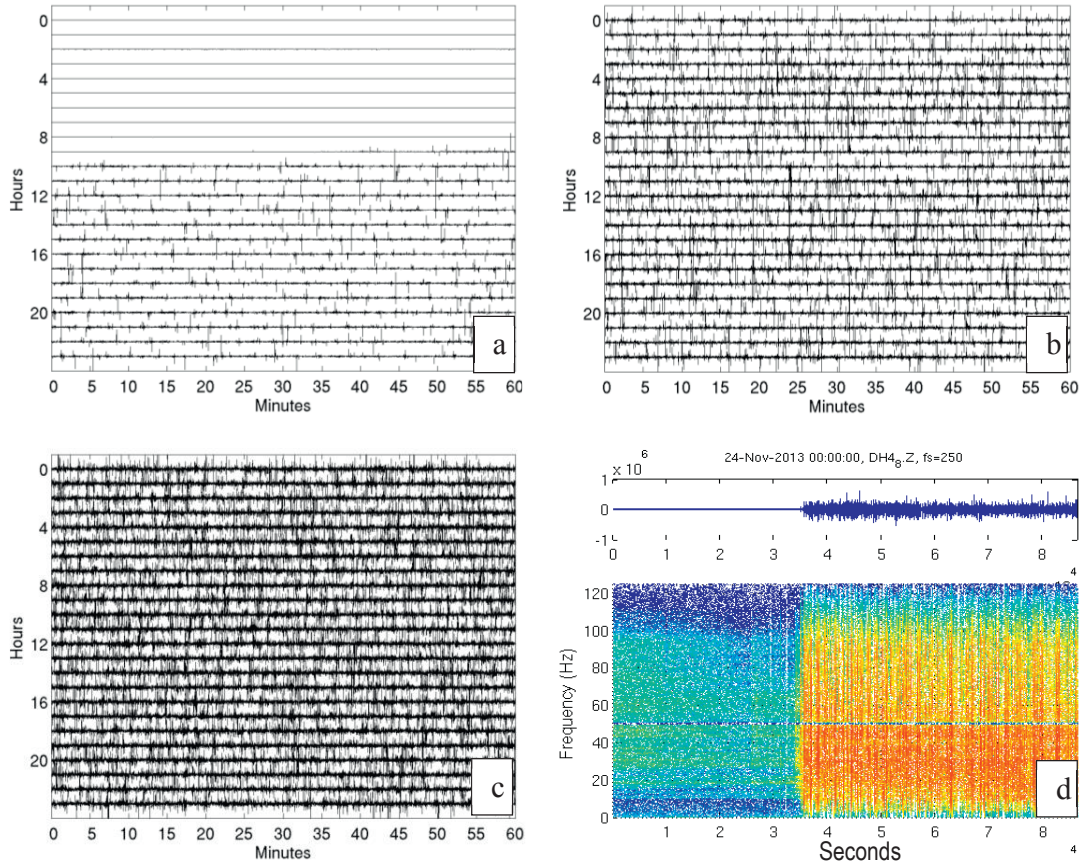

Fig. 2. Geophone 8 (vertical trace) within well Dh4; (a) heliogram 24.11.2013; (b) heliogram 28.11.2013; (c) heliogram 10.12.2013; (d) spectrogram showing the sudden start of noise in Dh4.

As can be seen in Fig.3, these signals do not represent electronic noise (e.g. spikes), but real seismic signals. They are most visible on the vertical component and strongly decrease in amplitude from bottom to top of the well. The propagation velocity is approximately 1.84 km/s (measured by the difference in arrival time). Also the frequency content of the data from the different geophones varies, which might result from differences in coupling of the sensors. We currently interpret these signals as Pseudo Rayleigh waves, more precisely tube waves, originating at the bottom of the well. During a subsequent site inspection, methane gas was detected leaking out of the well (resulting in the necessity to retrieve the geophone string in May 2014, such that the well could be closed and secured). Detection of both, biogenic and thermogenic methane at the CO2 Lab wellpark is common, as methane was also observed in most other deep wells. Seismogram observations within well Dh3 also show tube waves, likely due to degassing. At the current stage we cannot yet say for sure what caused the sudden onset of the seismic signals on the 24th of November; however, a sudden breakthrough of increased methane activity is a likely and currently discussed cause. Another interesting observation is that the number of these signals recorded in well Dh4 increases after the occurrence of regional earthquakes (Fig. 4). Such sudden increase of event activity followed by a slow decrease of the activity also points towards a relation of the event activity with methane ejection.

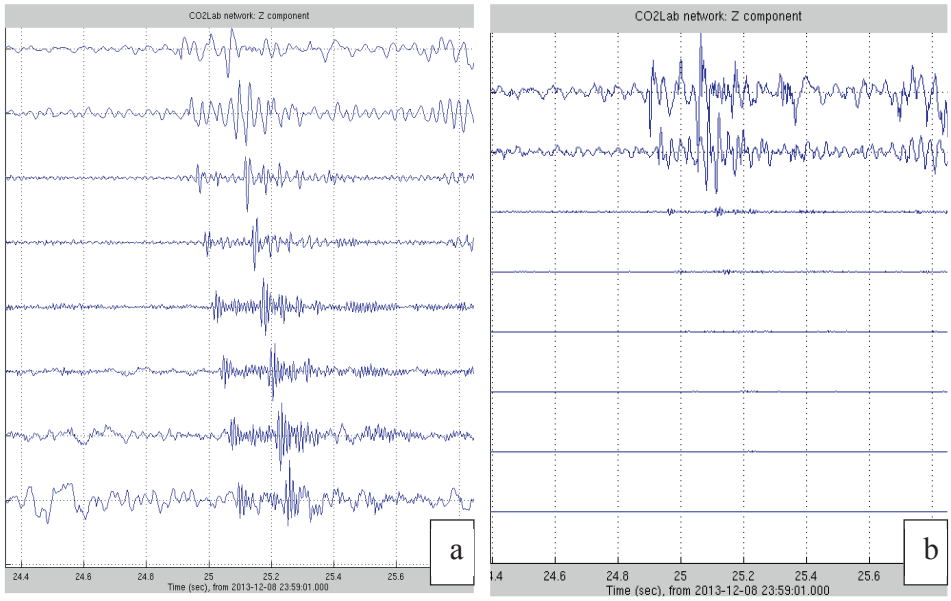

Fig. 3. Seismograms recorded in well Dh4; top trace: deepest geophone, at 540 m depth; bottom trace: shallowest geophone at 190 m depth; (a) recordings normalized to trace maximum; (b) traces normalized to overall maximum.

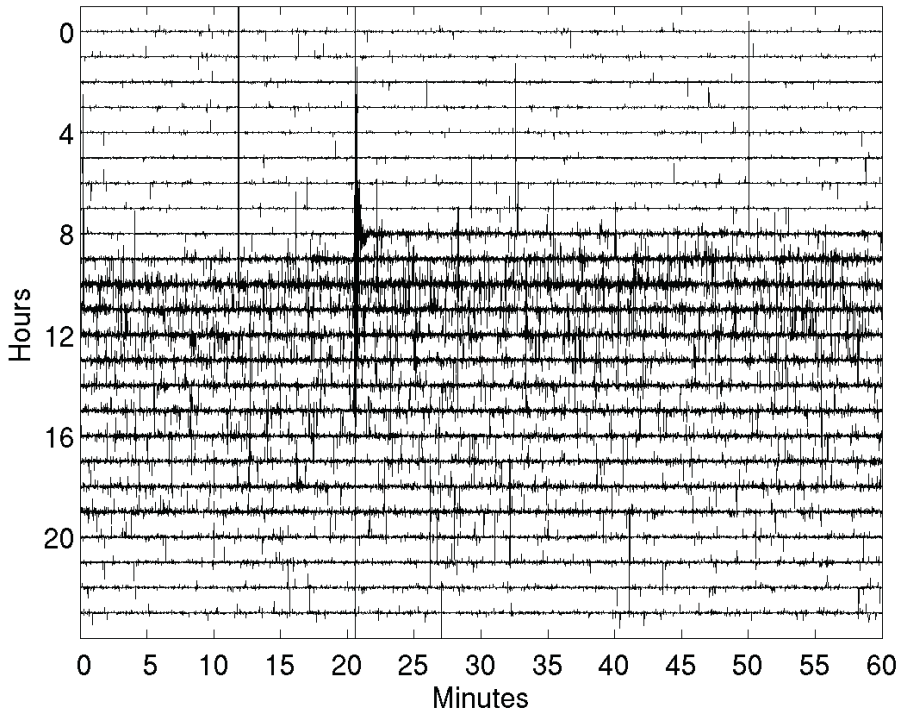

Fig. 4. Helicorder plot of seismograms recorded on geophone 6 within well Dh4. Note the increase in number of signals only seconds after the regional earthquake at 08:20h on 16th of December 2013 and then slowly decreasing activity.

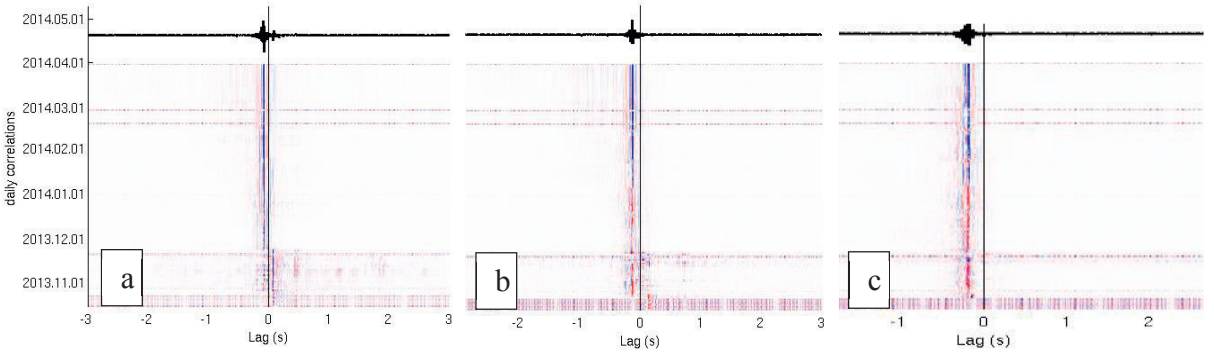

Fig. 5. Daily cross-correlation functions between sensors within well Dh4; top: stack of all traces; bottom: daily functions colour-coded; cross-correlations performed between traces recorded on (a) geophones 1 and 4, (b) geophones 1 and 6, (c) geophones 1 and 8

In order to compute cross-correlation functions of ambient seismic noise between stations, we employ the Whisper code [14]. The preprocessing includes decimation, assembling the data in one-day files, cutting traces for sub-treatments (in this case 30 minutes), filtering, clipping, spectral whitening and tapering [15]. Fig. 5 displays daily cross-correlation functions of sensors recording in well Dh4 filtered between 15 and 100 Hz starting October 2013 (bottom) until April 2014 (top). The stacked trace at the top is clearly asymmetrical exhibiting a negative lag time growing with distance between sensors (from left to right), indicating a dominance of signals travelling up the well (the tube waves). Interestingly, when signals recorded on geophones located in well Dh3 are cross-correlated with signals recorded in Dh4, the ambient noise in both wells correlates only for the upper sensors within Dh4 (geophones 1-5). Thus, we think that the fault zone shown in Fig. 1 decouples the noisefield in the overlying layers from the underlying layers.

4. Noise cancellation

Waveform data from the permanent seismic network are recorded in a hut at the Longyearbyen CO2 Lab, which provides a year-round, safe, temperature-controlled environment for the acquisition equipment. However, the hut also contains electrical equipment (heaters, power supplies, installations from other scientific experiments, etc.) that emits strong electromagnetic interference (EMI) and corrupts much of the data recorded on the installed geophones. Much of the interference consists of multiple sinusoids that are particularly troublesome for processing techniques that rely upon waveform correlation measurements. Sinusoids, of course, are highly correlated and, if persistent, can come to dominate long-term correlation measurements required in ambient noise tomography. Consequently, we desire to remove this interference by a post-processing step. We experimented with Widrow-Hoff cancellation (see e.g. [16]) using specially-recorded, independent samples of the interference. As a noise abatement strategy, cancellation is superior to notch filtering. Notch filtering introduces undesirable ringing in the waveforms, which can complicate the detection and interpretation of interesting transient microseismic signals. Cancellation is largely free of this kind of bias, but requires planning in its application and the dedication of acquisition channels to record noise reference waveforms.

The Widrow-Hoff algorithm operates by applying a filter to each EMI reference waveform, then subtracting the filtered traces from a target seismic data channel. The filters shape the reference waveforms to match interference in the target channel. Coefficients defining the filter response are selected to minimize the power of the residual in the subtraction operation. To function properly, the noise reference waveforms should be correlated with the interference in the target channel but be statistically independent of desired signal components in the target waveform.

During our experiment, 2 to 6 channels were dedicated to recording interference. Because 50 Hz interference

from the power line is ubiquitous in the data, one noise reference was a scaled recording of the power line waveform. For this recording, we constructed a simple voltage reduction circuit consisting of a step down transformer followed by a resistive voltage divider to fit the power line voltage range within the input limits of the recorders. A second reference was obtained by stringing a length of twisted pair around the room in the hut where the recorders were located. The intention here was to collect EMI from other sources in the room, such as the electric heater and switching power supplies.

Fig. 6 and Fig. 7 below are spectrograms of samples of the two reference waveforms (year 2014, day-of year 135, hours 14—16). In these plots power level is indicated by the intensity of the image, inverted so that dark pixels indicate high power and white pixels indicate no power. The plots display power as a function of time and frequency. The vertical axis is time increasing from the top of the image to the bottom; the total duration is two hours. The horizontal axis represents frequency on a linear scale, with frequency increasing from left to right. The left limit corresponds to 1 Hz and the right limit to 59 Hz.

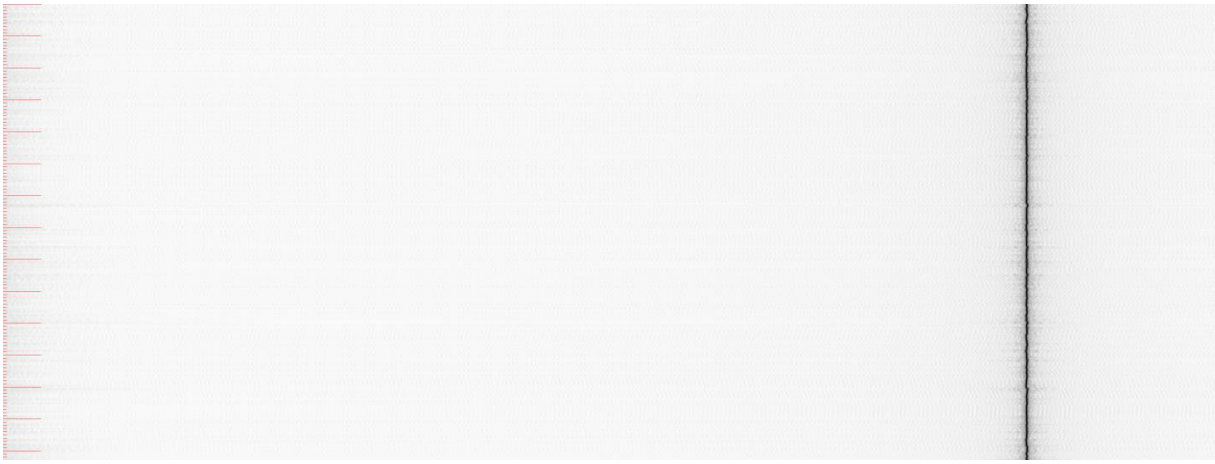

Fig. 6. Spectrogram of the signal recorded by the dedicated power line reference. The spectrum is completely dominated by the 50 Hz sinusoid forming the fundamental power line harmonic.

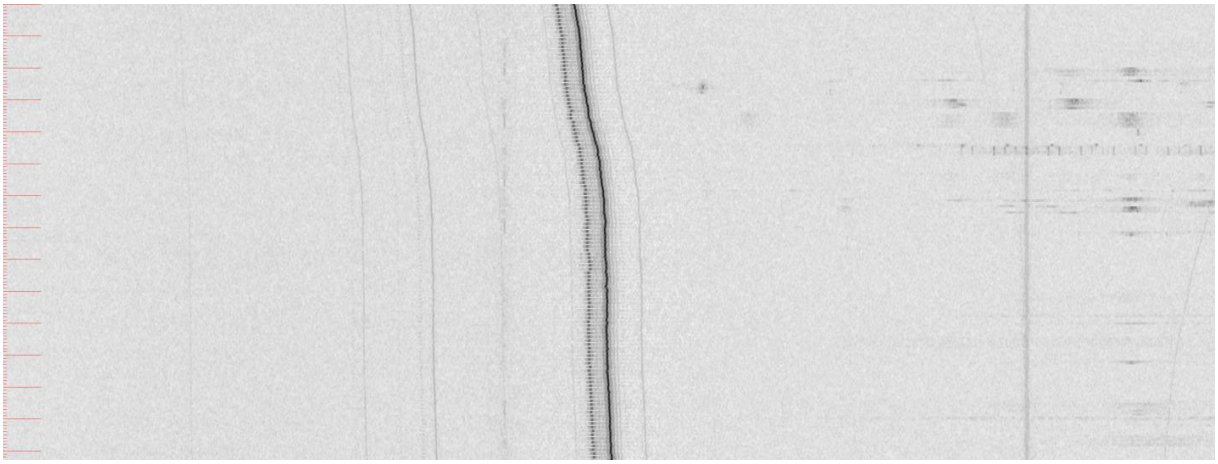

Fig. 7. Spectrogram of the second reference waveform, from a line running around the room containing the data acquisition equipment, attached to the walls near the ceiling. A strong nonstationary set of lines (i.e. lines with changing frequencies) is evident with a relatively weak contribution by the power line fundamental harmonic.

Fig. 6 is a spectrogram of the power line reference, and unsurprisingly, is dominated by a single line at 50 Hz. Note that, although this line is largely stable around 50 Hz, there are small frequency deviations from 50 Hz, probably due to changes in the load to the power grid as equipment is switched on and off. Because of these variations, it is not effective to generate a 50 Hz sinusoid with the correct amplitude and phase and simply subtract that theoretical waveform from the data as a cancellation method. Fig. 7 shows the spectrogram of the data from the noise pickup. This spectrum is dominated by a non-stationary source with multiple lines (some intermittent) drifting slowly in frequency. The source of this noise was not identified, though the electric heater in the room is a likely candidate. The 50 Hz line is also apparent in this record.

Fig. 8 is the spectrogram of a record from a data channel – station SH2, vertical component. Note that it has interference from both sources present in the references. The 50 Hz interference is particularly strong, as it is in much of the data. Fig. 9 displays the spectrogram of the cancellation residual obtained using just the power line reference. The 50 Hz line is effectively eliminated, leaving some broadband residual around 50 Hz. The spectrograms in Fig. 8 to Fig. 10 are autoscaled to bring up finer details as cancellation is applied; it is not the case that noise levels are increasing after cancellation.

Fig. 8. Spectrogram of the waveform from station SH2, vertical (Z) component

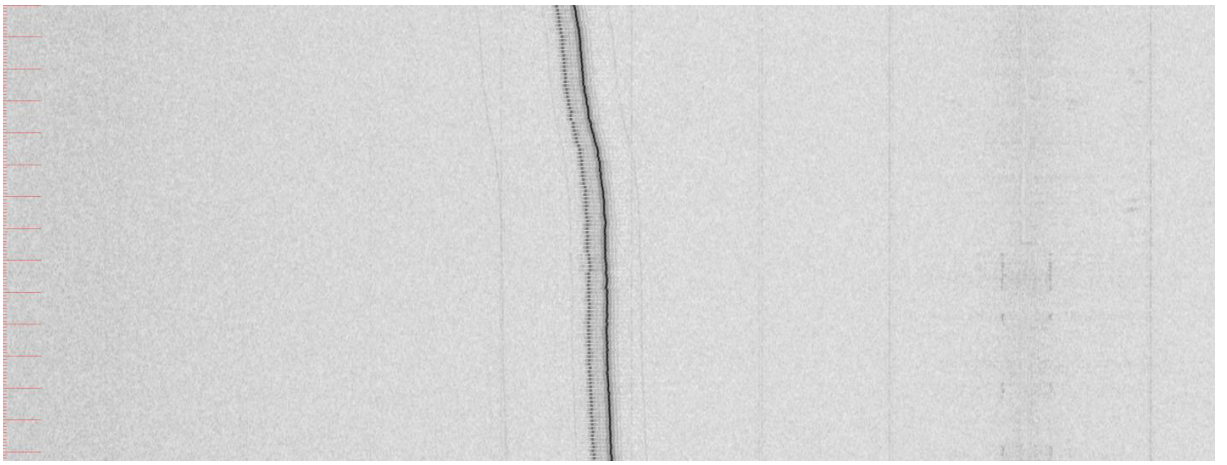

Fig. 9. Spectrogram of the SH2 Z residual after cancellation using the power line reference

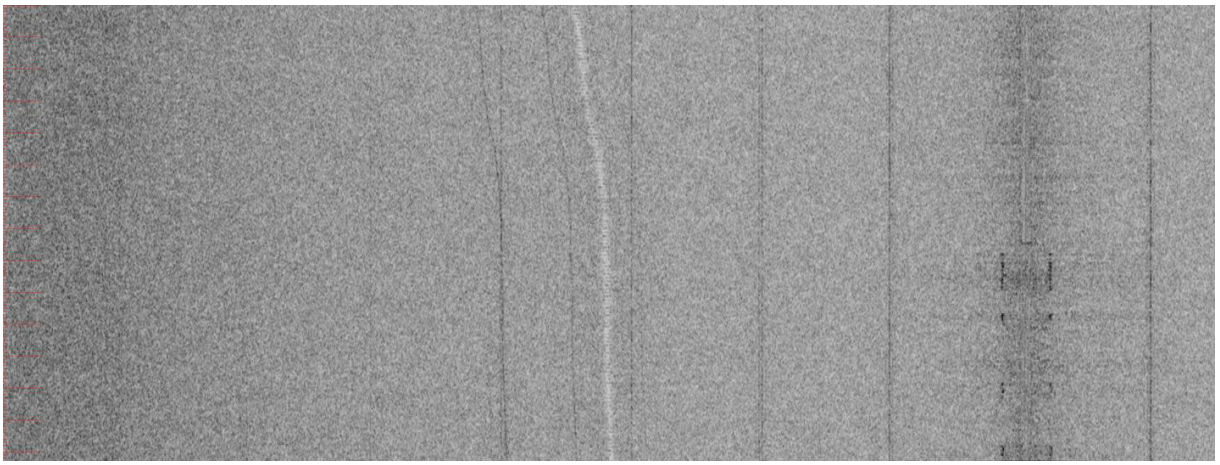

Fig. 10. Spectrogram of the SH2 Z residual after cancellation with both references

In Fig. 9, the variable-frequency interference dominates the residual, but faint lines spaced periodically at 6.25 Hz due to another independent noise source are apparent. Fig. 10 shows the spectrum after cancellation using both the power line and the pickup-noise references. Now the variable-frequency source has been suppressed, leaving principally the 6.25 Hz lines. We note that broadband background noise now contains most of the power in the spectrum. The power of this noise is largest at low frequency, suggesting that this noise is Earth motion, which is the actual "signal" that we seek in, for example, ambient noise correlation measurements.

5. Conclusions

According to [17] a tremendous amount of CO_2 - roughly an equivalent to the annual production of oil around the world - would need to be injected within geological subsurface storages to effectively reduce the current speed of global warming. A general threat to the integrity of CO_2 storage [18] is that even small- to moderate-sized earthquakes triggered by injection of such large volumes of CO_2 may cause leakage in the seal, thereby posing a severe limitation on the rate at which CO_2 can be injected. Thus, it is encouraging that most injection tests at the CO2 Lab did not produce microseismic events as opposed to e.g. the In Salah, Algeria, site [3]. Also note that the injection tests performed at the site so far are not representative neither in material injected (water) nor volumes; however, the amount of CO_2 produced by the coal power plant at Longyearbyen will be far less than at any industrial site, therefore local storage of CO_2 at the CO2 Lab is unlikely to be threatened by the risk of triggered seismicity.

Due to the extremely northern location of the CO2 Lab we encountered problems not typical for other monitoring sites. The climate is harsh on equipment; especially cabling was destroyed more than once during winter time (low temperatures probably rendering it brittle in combination with being invisible to vehicles and workers beneath snow and ice layers). Since the site is part of a nature protection area, constraints on the installation of instruments arose from environmental concerns. The recording equipment had to be stored in a hut, exposing the digitizers to a much higher degree to electromagnetic fields than experienced otherwise. In addition, the existence of permafrost turns the grounding of machinery into a very difficult and expensive task.

In addition, either the permafrost or the transition layer between permafrost and underlying rock acts as highly attenuating layer, decreasing the amplitudes of signals recorded on the shallow borehole sensors. Thus, deeper boreholes are strongly recommended to install sensors; on the other hand, the conditions in the High Arctic render drilling operations challenging [2].

Albeit the above described difficulties, new knowledge and guidelines for best practice containment monitoring using seismic methods in the Arctic could be developed. New methods for noise reduction are promising and they will improve the ability to detect microseismicity at even lower signal-to-noise ratios. The combination of using a high-frequency microseismic network for event location and noise correlation methods will be further developed. So far most deep borehole data is affected by more or less frequent occurrences of tube waves, likely originating from degassing. However, a more systematic analysis of the tube waves, will likely allow us to treat the tube waves further as a known and well-defined source and at the same time remove them when analyzing the data for event location purposes.

Acknowledgements

The work has been financed by Norwegian Research Council grants no. 189994 (SafeCO2 project) and 224880 (SafeCO2-II project). The projects have been sponsored additionally by our industry partners Lundin, Octio, READ and Statoil (SafeCO2) as well as Lundin, RWE DEA Norge and Statoil (SafeCO2-II). Further, we would like to thank the project staff not co-authoring this publication: S. Sikora (UNIS), I. Lecomte (NORSAR), M. Ohrnberger (University of Potsdam), F. Brenguier (ISTerre), B. Bohloli (NGI), C. Krawzcyk (LIAG) and U. Polom (LIAG). Fig. 1 has been prepared using QGIS (version 2.0.1. “Dufour”). G. Hillers acknowledges support from a Heisenberg fellowship from the German Research Foundation.

References

[1] Bergh, S.G., Braathen, A. & Andresen, A. 1997: Interaction of basement-involved and thin-skinned tectonism in the Tertiary fold-and-thrust belt, central Spitsbergen, Svalbard. American Association of Petroleum Geologists Bulletin 81, 637−661.

[2] Braathen A, Bælum K, Christiansen HH, Dahl T, Eiken O, Elvebakk H, Hansen F, Hanssen TH, Jochmann M, Johansen T., Johnsen H, Larsen L, Lie T, Mertes J, Mørk A, Mørk MB, Nemec W, Olaussen S, Oye V, Rød K, Titlestad GO, Tveranger J, Vagle K. The Longyearbyen CO2 Lab of Svalbard, Norway—initial assessment of the geological conditions for CO2 sequestration. Norwegian J Geol 2012: 92:353–76.

[3] Goertz-Allmann BP, Kühn D, Oye V, Bohloli B, Aker E. Combining microseismic and geomechanical observations to interpret storage integrity at the In Salah CCS site. Geophys J Int 2014:198(1):447-61.

[4] Oye, V., A Braathen, U Polorn, 2013. Preparing for CO2 storage at the Longyearbyen CO2 Lab: microseismic monitoring of injection tests. First Break, July 2013, Issue 7, Vol. 31.

[5] Lecomte, I., U. Polom, G. Sauvin, B.O. Ruud, H. Christiansen and G. Gilbert, 2014. Shear-wave Reflection-seismic Pilot Study at the UNIS CO2 Lab site, Longyearbyen, Svalbard, 76th EAGE Conference and Exhibition 2014 DOI: 10.3997/2214-4609.20141243

[6] Gilbert, G.W., 2014. Sedimentology and geocryology of an Arctic fjordhead delta (Adventdalen, Svalbard), Master Thesis, Department of Geosciences, University of Oslo, 2014.

[7] Oye, V., H. N. Gharti, D. Kühn, A. Braathen, 2010. Microseismic monitoring of fluid injection at the Longyearbyen CO2-Lab, Svalbard, in 'Cahiers due Centre Européen de Géodynamique et de Séismologie, Proceedings of the Workshop, “Induced Seismicity”, Nov 15-17, 2010, Luxembourg’, editors J. Ritter & A. Oth, 141 pages, ISBN 978-2-91989-709-4.

[8] Cornet, F., Helm, J., Poitrenaud, H., Etchecopar, A., 1997. Seismic and aseismic slipsinduced by large-scale fluid injections. Pure and Applied Geophysics 150 (3),563–583.

[9] Das, I., M.D. Zoback, 2013. Long-period, long-duration seismic events during hydraulic stimulation of shale and tight-gas reservoirs — Part 1: Waveform characteristics, Geophysics, Vol. 78, No. 6, doi:10.1190/GEO2013-0164.1

[10] Campillo M. Phase and correlation in ‘random’ seismic fields and the reconstruction of the Green Function. Pure Appl. Geophys 2006:163: 475–502.

[11] Sens-Schönfelder C, Wegler U. Passive image interferometry and seasonal variations of seismic velocities at Merapi Volcano, Indonesia. Geophys Res Lett 2006:33.

[12] Wegler U, Nakahara H, Sens-Schoenfelder C, Korn M, Shiomi K. Sudden drop of seismic velocity after the 2004 Mw6.6 mid-Niigata earthquake, Japan, observed with Passive Image Interferometry. J Geophys Res 2009:114.

[13] Shapiro NM, Campillo M, Stehly L, Ritzwoller M. High resolution surface wave tomography from ambient seismic noise. Science 2005:307:1615-18.

[14] Briand X. Whisper code provided by Whisper project FP7 ERC Advanced grant 227507 (WHISPER). Accessible at http://code-whisper.isterre.fr/html/index.html.

[15] Albaric J, Hillers G, Kühn D, Harris D, Brenguier F, Ohrnberger M, Oye V. Ambient seismic noise analysis from array and borehole networks in Svalbard, Norway. Fifth EAGE Passive Seismic Workshop, Extended Abstracts 2014.

[16] Haykin S. Adaptive Filter Theory, 4th ed. New Jersey: Prentice-Hall; 2008.

[17] Snieder R, Young T. Facing major challenges in carbon capture and sequestration. GSA Today 2009:19(11):36-7.

[18] Zoback MD, Gorelick SM. Earthquake triggering and large-scale geologic storage of carbon dioxide. Proc Nat Academy Science 2012:109(26):10164-68.